ORIGINAL ARTICLE

New data on relevant ancient Egyptian wooden artifacts: Identification of wooden species and study of the state of conservation with multidisciplinary analyses

Neveen Geweely[1] | Amira Abu Taleb[1] | Shimaa Ibrahim[1,2] |
Paola Grenni[3] | Giulia Caneva[4] | Giulia Galotta[5] |
Medhat Abdallah[6] | Dina Atwa[2] | Jasper Plaisier[7] |
Federica Antonelli[8]

[1]Faculty of Science, Botany and Microbiology Department, Cairo University, Giza, Egypt

[2]Ministry of Antiquities, Museums sector, Grand Egyptian Museum, Cairo, Egypt

[3]Water Research Institute (IRSA), National Research Council, (CNR), Rome, Italy

[4]Department of Science, University Roma TRE, Rome, Italy

[5]Ministry of Culture (MIC), Biology Laboratory, Istituto Centrale per il Restauro (ICR), Rome, Italy

[6]Conservation of Saqqara storerooms, Ministry of antiquities, Giza, Egypt

[7]Elettra Sincrotrone Trieste SCpA, Basovizza, Trieste, Italy

[8]Department for Innovation in Biological, Agro-Food and Forestry Systems (DIBAF), Tuscia University, Viterbo, Italy

Correspondence
Neveen Geweely, Cairo University, Faculty of Science, Botany and Microbiology Department, Giza, 12613, Egypt.
Email: ngeweely@cu.edu.eg; ngeweely@sci.cu.edu.eg

Abstract
Wood species identification and characterization of its weathering processes are crucial steps in the scientific approach of conservation of wooden cultural heritage. Many precious wooden objects of ancient Egypt are largely present in museums, nevertheless relatively little information is available concerning the nature of timber used and on their status of conservation. To address this gap, the wooden species of three relevant archaeological wood objects (statue, box, and coffin) arising from different Egyptian archaeological sites dated from the Old Kingdom (2,686–2,181 BC) to New Kingdom (1,550–1,069 BC) were deeply studied. Five hardwood and softwood species were identified belonging to *Tamarix mannifera*, *T. gennessarensis*, *Ficus sycomorus*, *Vachellia nilotica*, and *Cedrus* sp. Such data confirmed the recurrence of *Vachellia* and *Tamarix* among the most common timbers found in ancient Egypt. Scanning electron microscope, Fourier transform spectroscopy, and synchrotron x-ray radiation diffraction were conducted to evaluate the archaeological wood deterioration. The formation of microcracks, biological degradation patterns (fungal colonization), or chemical characterization (accumulation of salts on and in-between wooden cells) were detected. SEM micrographs showed the presence of fungal hyphae and conidial spores on the wooden cells.

Significant changes in the chemical wood composition and decrease in the crystallinity index were detected.

INTRODUCTION

Thanks to some characteristics, such as durability and workability, wood was highly valued in ancient Egypt. Despite the paucity of indigenous wood species that allowed obtaining timber of sufficient dimensions, this material was widely used to make a broad range of artifacts: ships, statues, wooden boxes, and painted decorated coffins (Creasman, 2014). Its importance is testified by several scenes found in tomb paintings showing woodcutters intent on felling trees or removing branches from trunks (Gale et al., 2000). Ancient sources, like Theophrastus and Pliny, talk about evidence of the native species used in ancient Egypt. Acacias, sycomore fig and persea have been reported as the most used wood, together with different species of palm (Meiggs, 1982). Anyway, an intensive use of foreign timbers has been also known. Different conifers (cedars, pines, firs, and junipers), ebony, oak, elm, and many others were imported from Lebanon, Syria, North Africa, and other regions of the Mediterranean area (Creasman, 2014; Gale et al., 2000). It must be underlined that in antiquity often more than one wooden species was identified with the same name, so the attribution of ancient sources should not be considered as accurate. From the work of Lucas (1959) onward, the identification of wooden species through microscopic analyses has been more systematically performed on Egyptian artifacts. These studies provide a base for a more comprehensive understanding of use and commerce of wood in ancient Egypt.

Thanks to the favorable conservation conditions provided by the Egyptian dry climate, a huge amount of wooden artifacts have survived to the present days (Caneva et al., 2008). The extraordinary Egyptian finds that came to light after so long time frequently reveal signs of alterations due to the concomitance of different causes both of abiotic (e.g., excessive temperatures and thermal stress) and biotic type. The fungal colonization has often been recorded in wooden objects and explained by the access and occasional retention of water in hypogeal chambers and pits preserving wooden finds in archaeological sites with microaerophilic conditions if sealing was partially lost (Blanchette et al., 1994; Nilsson & Daniel, 1989). During the post-excavation storage and repair phases, archaeological wood is exposed to a significant risk of biological deterioration (Geweely, 2022).

Because these artifacts constitute an important part of the worldwide cultural heritage, the identification and characterization of wooden species used to realize them together with the evaluation of the deterioration degree are crucial for their characterization and correct preservation (Blanchette, 2003). Nevertheless, relatively little information is available concerning the type of timber used and on their state of conservation and further information on this topic is still relevant. Identification of ancient wooden species can be a challenge when considering the great variety of wooden materials used in the past and the ageing and degradation phenomena affecting the material appearance and its structural integrity (Timar et al., 2010). The microscopic recognition of wood morphological features by different microscopical tools (stereo, optical, and electron microscope) is an integral part of the identification and classification process (Richter & Dallwitz, 2000). Furthermore, microscopic observation allows to evaluate the degradation state of wood cell walls and the eventual presence of biodeteriogen microorganisms. Optical microscopy has routinely been used in the wooden species identification and

widely proved its utility in the degradation phenomena characterization (Baas & Wheeler, 1998; Giachi et al., 2016; Romagnoli et al., 2018; Schwarze, 2007; Cartwright, 2015). Scanning electron microscopy (SEM) proved to be highly considered in its application for cultural heritage studies, and in particular in archaeological wood because it provides information on the features associated with different wood degradation phenomena (Blanchette, 2000; Cartwright, 2015, 2019, 2020). SEM can be an optimal tool for the study of the structure of degraded wood at both high and low magnification with excellent detail resolutions (Hamed et al., 2012). Due to the rarity and value of cultural heritage objects, obtaining samples for physical and chemical analysis by destructive methods (e.g. cutting, scraping, or drilling) is generally unacceptable. Consequently, SR-XRD has been used to measure the crystallinity of cellulose, which is an important indicator of wood decay. Moreover, Fourier transform infrared microscopy (FTIR) has been used to study the changes in wood chemistry compounds (cellulose- hemicellulose- lignin) following decay. These compounds have characteristic absorption spectra in FTIR analysis (Tamburini et al., 2017).

The present work aimed to expand the knowledge on woods used in artifacts from the Egyptian Old Kingdom and New Kingdom through the characterization and identification of three relevant wooden artifacts. Microscopic tools were used for evaluating the degradation patterns; the chemical changes in wood main components (cellulose, hemicelluloses, and lignin) were investigated using FTIR and XRD. The new data will be useful for improving the information about ancient technology in the Mediterranean area from the Old Kingdom (dated about five millennia) to the late period.

MATERIAL AND METHODS

Artifacts

The present study involved three pharaonic wooden objects belonging to different periods. The wooden statue (ID number SR2/15969) belongs to the Old Kingdom (Figure 1a). It was discovered by the Egypt Exploration Society; it was found in a poor state of preservation in the Memphite region (North of Saqqara-Giza-Egypt). The coffin (ID number SR3/643) is an anthropoid artifact with the cartonnage mummy of the Nespahettawi, son of Neskhonsupahred (Figure 1b). The wooden box of Padimen son (ID number CG5028) is a container for canopic jars (Figure 1c, d). The coffin and the wooden box were both discovered in the Deir el-Bahari archaeological site and belong to the New Kingdom. All three archeological objects are now preserved in the Egyptian Museum of ELTahrir, Cairo, Egypt.

Sampling

Small samples (<2 × 2 × 2 mm) were collected by sterile scalpel from deteriorated parts on the artifacts to perform microscopic analyses. For items made of more than one piece (i.e., the wooden box and the wooden coffin), sampling was carried out on each part.

Wood species identification

Wood micromorphological features highlighted by microscopical observations were used to identify wooden species. In particular, wood databases (Richter & Dallwitz, 2000; Wheeler, 2011) and specialized publications (Crivellaro & Schweingruber, 2013; Gale & Cutler, 2000; Waly, 1999) were used to perform identifications.

FIGURE 1 The three studied wooden objects Notes: (a) Statue (L 127 cm, W 47 cm); (b) coffin with cartonnage mummy of Nespahettawi, son of Neskhonsupahred (L 179 cm, W 55 cm); (c) and (d) front and backside of Padimen son box (L 43.5 cm, W 39 cm)

Optical microscopy

Wooden samples were first examined with a stereomicroscope (M205C, LEICA) at different magnifications at the biology laboratory of the Central Institute for Restoration (ICR) in Rome (Italy). The samples were then cut either by hand with razor blades or by freezing microtome (Cryostat CM 1900, LEICA), obtaining thin sections (10–20 μm thick) in the three anatomical planes (transverse, tangential longitudinal, and radial longitudinal). In some cases, before cutting, the wood was immersed in water for few minutes to soften tissues. Sections were soaked in water under lead loads for 24 hours and then mounted on slides with a drop of glycerol. If necessary, part of the sections was stained with an aqueous solution of 1% (w/v) methylene blue in 50% lactic acid or with safranin 1% (w/v) in a water–ethanol 50:50 ratio to highlight the occurrence of microorganisms.

In some very fragile and brittle wood specimens (e.g., wooden statue), sectioning was almost impossible to perform, and an embedding treatment was required. Consequently, to maintain the sample integrity during cutting operations, an acrylic-based thermoplastic resin was used (Galotta, 1999). The resin was composed in butyl methacrylate and methyl methacrylate (10:1 ratio), and in 1% (w/v) benzoyl peroxide (as the catalyst). Before wood embedding, a part of the resin was pre-polymerized by heating at 65–70°C on a hot plate with a magnetic stirrer for about 60–90 min.; it was then cooled on ice and stored at 4°C. For the embedding procedure, wood specimens were first soaked in a mixture of butyl-methyl methacrylate 10:1 catalyst-less resin for 1 hour. They were subsequently put in starch capsules filled with

pre-polymerized resin and let polymerize in a oven at 60°C overnight. Because wood was already in a dry state, no dehydration steps were required. After hardening, samples were cut using sliding microtome to obtain thin sections. Resin embedded sections were treated with ethanol to favor adhesion to the glass slide and mounted with glycerol.

All sections were examined using light microscopy (Axio Imager M2, Zeiss) equipped with digital camera. Images were acquired and processed by Zen 2.3 Pro (Zeiss). Microbial decay was detected using both bright field and polarized light.

Wooden deterioration analyses

Scanning electron microscopy (SEM)

SEM observations were carried out at the National Research Centre (NRC), Cairo, Egypt, by using the microscope QUANTAFEG 2250, operating at 15 Kv. No preparative technique was used to treat the samples in order to not interfere with the wood surface.

Fourier transform infrared spectroscopy (FTIR)

FTIR analysis was carried out using Bruker Vertex 70 FTIR spectrometer equipped with an attenuated total reflectance (ATR) unit ~~was used~~ at the Research Center for Restoration of Antiquities in Cairo, Egypt. Spectra were measured at 4 cm^{-1} resolution and 16 scans were recorded per sample with spectra in the range of 4,000–400 cm^{-1}.

X-Ray diffraction

The crystallinity of cellulose was performed by X-ray diffraction, as it is recognized that this tool is the most appropriate. High-energy x-ray diffraction was performed at the MCX beamline of Elettra Synchrotron (Trieste, Italy) to determine the crystallinity of cellulose with minimal sample preparation requirements. The measuring energy was 13 KeV at room temperature with a 2θ range from 2° to 40° with a transmission experimental set up (Plaisier et al., 2017). Segal method is the most widespread and was applied in this study, it was used to characterize the crystallinity of cellulosic samples (Huang et al., 2012; Picollo et al., 2011). The crystallinity of cellulose X was calculated by:

$$X = 100\, x \frac{I\,(200) - I\,(am)}{I\,(200)}$$

Where: (X) expresses the crystallinity of cellulose, I $_{(200)}$ is the height of the (200) peak, and I$_{(am)}$ is the height of the minimum between the (200) and (110) peaks. The crystallinity obtained using this method is dependent on crystallite size and cellulose allomorph (Ju et al., 2015).

RESULTS AND DISCUSSION

Wood species identification

The analyses of micromorphological features of wood by optical and scanning electron microscopy allowed identifying five different wooden species (Table 1).

Artifact		Wood species
Statue		Acacia, cfr. *Vachellia nilotica* (L.) Willd. Ex Delile
Box of Padimen son	Body	Sycomore, *Ficus sycomorus* L.
	Connection	Tamarisk, *Tamarix mannifera* (Ehrenb.) Bunge
Anthropoid coffin	Body	Cedar, *Cedrus* sp. A. Rich.
	Connection	Tamarisk, *Tamarix gennessarensis* Zoh.

Vachellia nilotica (L.) P.J.H.Hurter & Mabb. (BABUL ACACIA) synonym: *Acacia nilotica* (L.) Willd. Ex Delile, family Fabaceae (Mimosoideae clade)

The study of the fragment of the wooden statue allowed the identification of the species *V. nilotica*. The diffuse-porous wood was characterized by growth ring boundaries indistinct or absent, vessels solitary or in multiples, less than 20 per square millimeter in frequency (Figure 2a). The tangential diameter of largest vessel was about 150 μm. Simple perforation plates, alternate intervessel pits (7–10 μm in diameter), and vestured pits were present. Heartwood vessels were characterized by the presence of dark deposits. Axial parenchyma was vasicentric, aliform lozenge-aliform, and confluent. Thick-walled fibers and gelatinous walls fibers were observed. In tangential sections, prismatic crystals were observed (Figure 2b I). The rays were pluriseriate (<10 seriate), with a height just exceeding 1 mm, exclusively composed of procumbent cells (Figure 2c I).

A. nilotica was recently reclassified based on phylogenetic studies (Boatwright et al., 2014; Haddad, 2011; Kyalangalilwa et al., 2013). Consequently, it is necessary to refer to this species with the new accepted name of *V. nilotica* (L.) P.J.H. Hurter & Mabb.

The plant is native to the drylands of tropical Africa and western Asia, eastward as far as India, Myanmar, and Sri Lanka. In Africa it occurs from Senegal to Egypt, where it grows beside the Nile, to open habitats such as savannas, and southward through eastern Africa to Mozambique and South Africa, and the Indian Ocean islands (Bouchenak-Khelladi et al., 2010; Fagg & Mugedo, 2005; Liphschitz, 1998; Orwa et al., 2009).
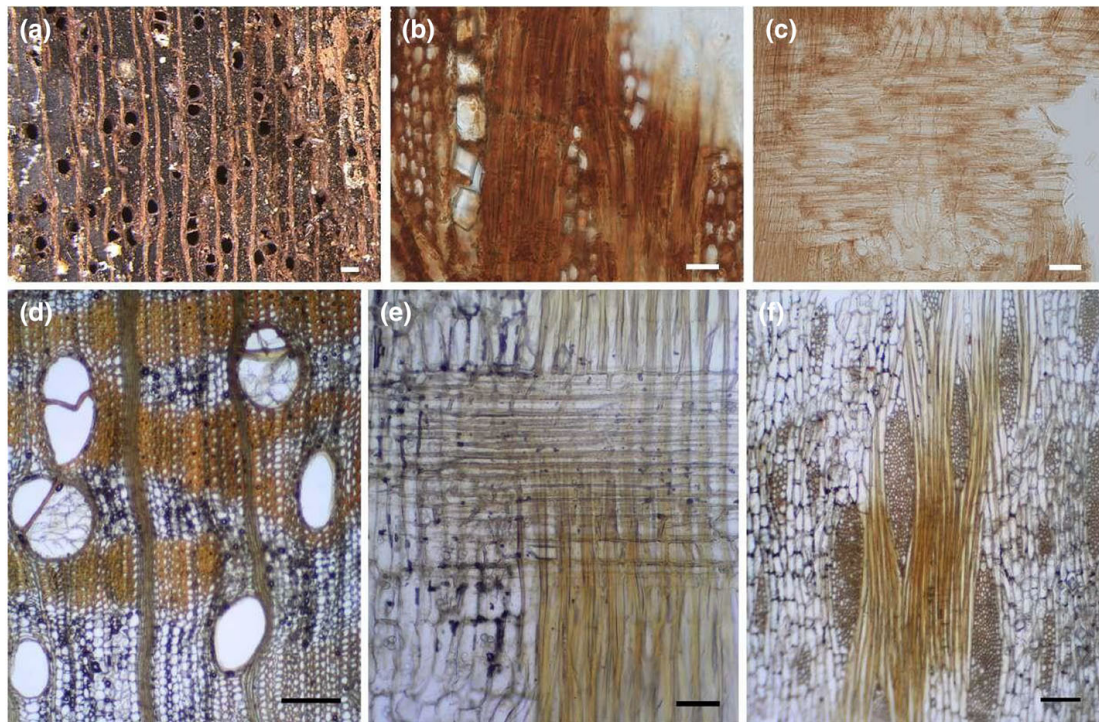
The wood is characterized by hardwood red to brown in color, often darkening upon exposure, and distinctly demarcated from the white-yellowish sapwood. Although the texture is not fine, thanks to the thick-walled fibers, acacia wood is very compact. It is strong and durable, hard and heavy with a high density (Fagg & Mugedo, 2005; Giordano, 1997).

Suitable for growing in arid environments like Egypt, the species was widely spread, and acacia wood is very well represented in a vast range of ancient Egyptian artifacts (Cartwright, 2019; Cartwright & Taylor, 2008; Gale et al., 2000; Gale & Cutler, 2000; Lucas, 1959; Melchiorre et al., 2020). Its use is largely reported by ancient sources. Meiggs states that acacia was the most extensively utilized species and cites both Herodotus, reporting that the "baris" (a common type of cargo on the Nile) was built with relatively small pieces of acacia fitted together like blocks, and Theophrastus, who affirmed that from acacia trees could be cut great resistant beams, suitable for ship hulls construction (Crivellaro & Schweingruber, 2013). Indeed, most authors agree that acacia was the most used species for built ships and boats, together with cedar and tamarisk (Creasman, 2014).

F sycomorus L. (Sycomore fig), family Moraceae

The body element of the wooden box of Padimen son was made of sycomore fig. The wood was diffuse porous, characterized by growth ring indistinct or absent. The vessels, solitary or in

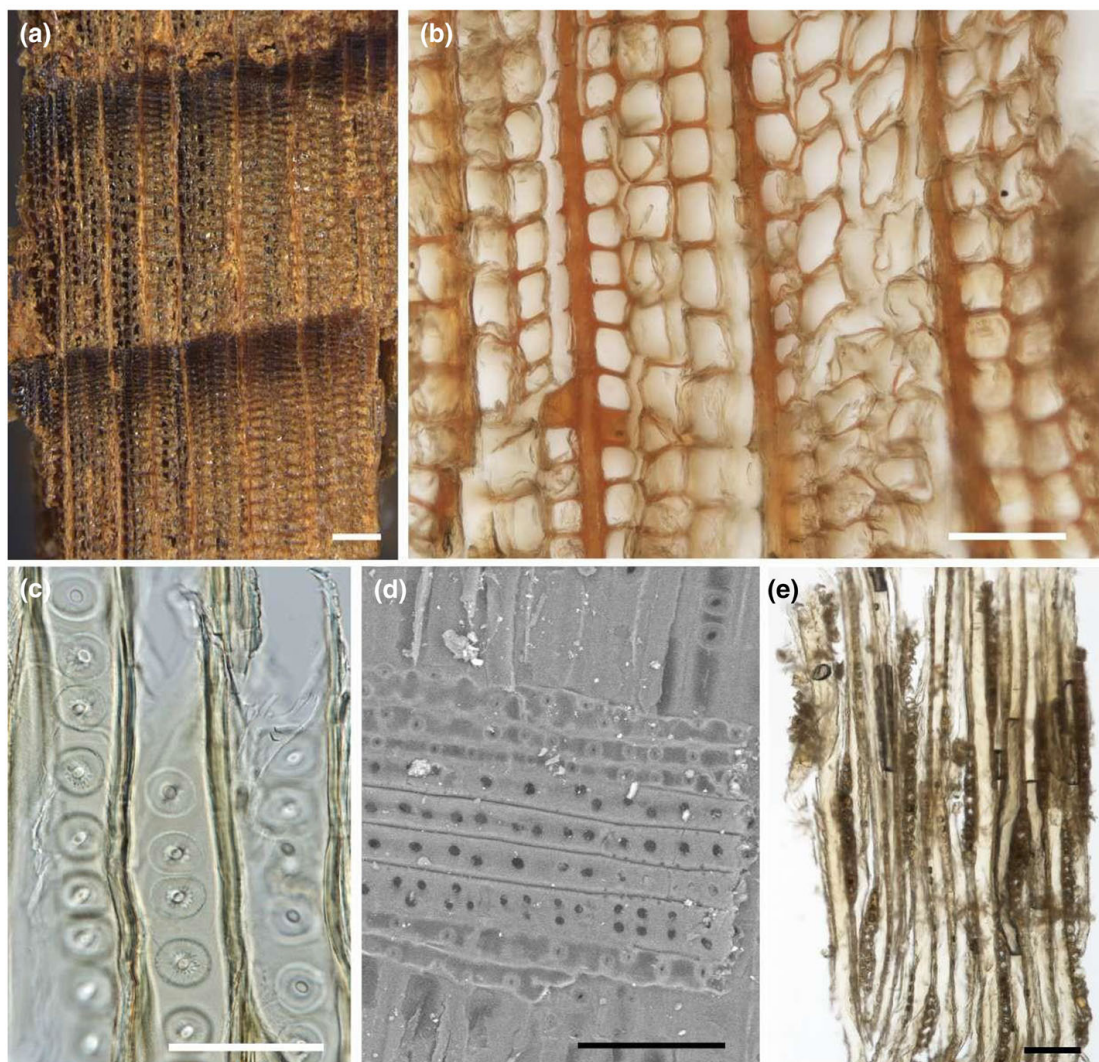NEW DATA ON RELEVANT ANCIENT EGYPTIAN WOODEN ARTIFACTS: IDENTIFICATION OF WOODEN
SPECIES AND STUDY OF THE STATE OF CONSERVATION WITH MULTIDISCIPLINARY ANALYSES

7

F I G U R E 2 **I** (a-c) wooden statue (ID number SR2/15969): Acacia, Vachellia nilotica. (d-f) Box of Padimen son (ID number CG5028), body: Sycomore, Ficus sycomorus L. (a) Transverse section micrograph at stereo microscope showing diffuse-porous wood, vessels solitary or in multiples, tangential diameter of largest vessels 150 μm ca. (b) Tangential section, optical microscope, crystals in rays. (c) Radial section, optical microscope image, ray composed of procumbent cells. (d) Optical micrograph, transverse section showing vessel having diameter 100–200 μm, solitary or in radial multiple of 2 cells. (e) radial section, optical microscope. Ray is made of procumbent cells with 2 rows of upright and square marginal cells. Axial parenchyma arranged in tangential bands. (f) Tangential section, optical microscope, showing rays 3–10 seriate. Scale bars: a, d, f = 200 μm, b = 20 μm, c = 50 μm, e = 100 μm. **II** anthropoid coffin (ID number SR3/643), body: Cedar, Cedrus libani A. Rich. Micrographs obtained with different techniques. (a), (b) Transverse sections. Homoxylous wood without resin ducts. (a) Stereomicroscope. (b) Optical microscope. (c) (d) Radial sections. Axial tracheid's pits with scalloped tori. Presence of ray tracheids, cross-field pitting taxodioid, or piceoid. (c) Optical microscope. (d) SEM. (e) Tangential section. Low, uniseriate parenchyma rays without horizontal resin canals. Scale bars: a = 200 μm, b, d, e = 100 μm, c = 50 μm. **III** box of Padimen son (ID number CG5028), connection: Tamarisk, Tamarix mannifera (Ehrenb.) Bunge. Optical microscope micrographs. (a) Transverse section showing vessel having diameter 100–200 μm, frequency < 20/mm^2, pluriseriate rays. (b) and (c) Tangential sections showing larger rays commonly 4–10 seriate or more. (b) Bright field. (c) Radial section. Rays with up to 4 rows of square cells, alternate minute intervessel pits. (d) Tangential section observed under polarized light, prismatic crystals absent. Scale bars: a = 200 μm, b, c = 100 μm, d = 50 μm.

radial multiple (mainly of 2) (Figure 2I d), had mean tangential diameter of lumina 100–200 μm and alternate intervessel pits. The axial parenchyma was arranged in tangential bands more than three cells wide. The observed rays were uniseriate and pluriseriate (larger rays 3- to 10-seriate), made up of procumbent cells with 1 to 4 rows of upright and square marginal cells (Figure 2I e-f).

Sycomore fig native range extended from Africa to Syria. Its present distribution comprises Egypt, Syria, the Arabian Peninsula, the Cape Verde Island, South Africa, and Namibia. The timber obtained from this species is pale, light, fibrous, coarse, and of poor quality, with rather low density (Crivellaro & Schweingruber, 2013; Gale et al., 2000; Giordano, 1981). Due to lightness, as long as good availability of timber, sycomore fig was extensively used in ancient Egypt for a wide range of objects including coffins, statues, mummy portraits and painted panels (Abdrabou et al., 2017; Cartwright, 2019, 2020; Gale et al., 2000; Killen, 2017; Lucas, 1959; Meiggs, 1982), boats, and ships (Creasman, 2014; Giachi et al., 2016).

Cedrus sp. (cedar), family Pinaceae

The micromorphological features observed for the body element of the wooden anthropoid coffin (ID number SR3/643) allowed identifying cedar. The wood was characterized by distinct growth ring boundaries without axial resin canals (Figure 2II a, b). Tracheid pitting was mostly uniseriate in radial walls, and bordered pits were present also on the tangential walls of the axial tracheids. The scalloped tori, typical of this genus, were observed for bordered pits (Figure 2II c). Rays were uniseriate, with cross-field pitting taxodioid or piceoid (1–2 per cross-field), characterized by the presence of ray tracheids (Figure 2II d), very low (up to 4 cells), or medium (5 to 15 cells) (Figure 2II e).

Based on the reported micro-anatomical features, it is difficult to distinguish among the three species of the genus *Cedar*, two of which are indigenous of Mediterranean basin (*C. libani* A. Rich and *C. atlantica* [Endl.] Manetti ex Carrière) and one with a native range from NE Afghanistan to W Nepal and NW India (*Cedrus deodara* [Roxb. Ex D.Don] G.Don). The native range of *C. libani* is from Turkey to Lebanon, Cyprus, whereas *C. atlantica* originates from N - N Central Morocco to N Algeria.

Although Killen, 2017 affirmed that *C. libani, C. atlantica,* and even *C. deodara* were used in ancient Egypt, Gale et al., 2000 reported no evidence of ancient commercial wood trades among Egypt and Morocco or central Asia and assume that only *C. libani* was used. On the

NEW DATA ON RELEVANT ANCIENT EGYPTIAN WOODEN ARTIFACTS: IDENTIFICATION OF WOODEN
SPECIES AND STUDY OF THE STATE OF CONSERVATION WITH MULTIDISCIPLINARY ANALYSES

9

III

FIGURE 2 (Continued)

other hand, the Lebanese commercial route was so common, since the predynastic period, that the Egyptian sea-going vessels were also known as 'Byblos boats', from the name of the Lebanese port town entrepôt of Mediterranean and Aegean commerce (Jenkins & Ross, 1980). Political and commercial relations between Cyprus and Egypt easily allowed the cedar timber import from that island (Meiggs, 1982). Therefore, the hypothesis of the use of *C. libani*, or of its variety *brevifolia*, endemic to Cyprus should be taken into account as the most likely.

Cedar timber has reddish-brown hardwood, distinctly demarcated from sapwood. It is reported as straight grained and fine textured, with low-medium density, it can be easily worked until it reaches a good polish (Giordano, 1997). Hardwood is very durable, also for outdoor uses (Nardi Berti et al., 2006). Killen distinguishes the timber of *C. libani* from that of the other species of the genus describing it as of poorer quality, soft, with a rough grain, and subject to

shrinkage during natural seasoning (Killen, 2017). Indeed, in general, it must be taken into account that timber quality, especially its density, highly depends on site growth conditions (Nardi Berti et al., 2006).

Several wooden objects are described as cedar made in museum catalogs and excavation reports but not all attributions should be considered as correct because the word cedar is (and so was also in Greek and Roman period) loosely used to define different trees that are not actual cedar (Gale et al., 2000). Real cedar wood was surely used in ancient Egypt for quality coffins, its high cost linked to the import from other counties, its attractive aromatic scent, and its resistance to rot and insect attacks made it a particularly valuable material (Gale et al., 2000; Giachi et al., 2020; Meiggs, 1982; Nisbet, 1982). It was also used to make monumental doors, ships, burial boats, ship models, coffins, headrests, mummy portraits, and painted panels (Cartwright, 2019, 2020; Creasman, 2014; Creasman, 2015; Fadl et al., 2013; Gale et al., 2000; Gale & Cutler, 2000; Giachi et al., 2016; Meiggs, 1982).

Tamarix spp. (tamarisk), family Tamaricaceae

The two connection elements of the Padimen son Box and the Anthropoid coffin were made of tamarisk wood belonging to two different species.
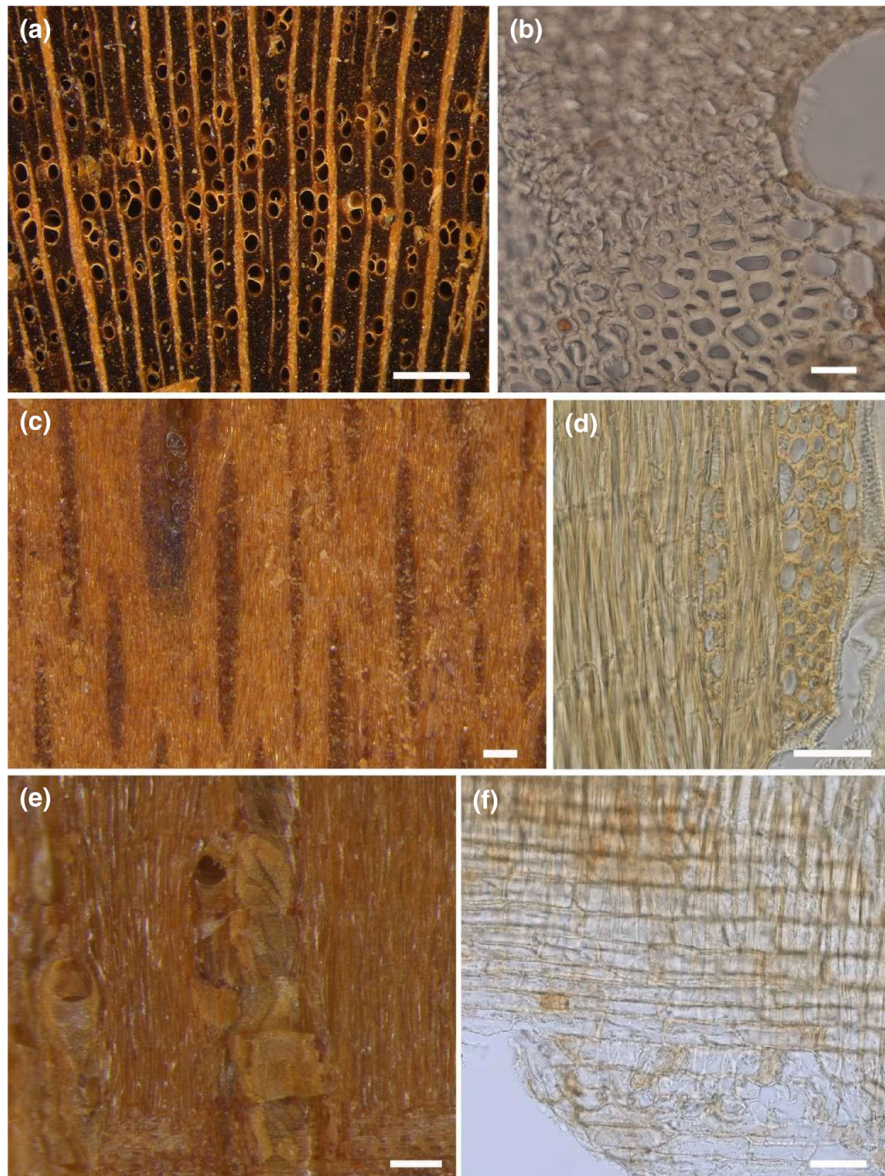
Following the Inside Wood database identification key (Wheeler, 2011), the connection of the wooden box of Padimen son was identified as *T. mannifera* Ehrenb. ex Bunge (sin = *T. senegalensis* D.C.).

The semi-ring porous wood was characterized by growth ring boundaries indistinct or absent. The vessels, solitary or in multiples of 2–4, were commonly arranged in tangential bands and in clusters, with a frequency of 5–20 vessels per square millimeter. The mean tangential diameter of vessel lumina was 100–200 μm (Figure 2III a). The larger rays were commonly 4 to 10 seriate or more (Figure 2III b) with height exceeding 1 mm. In radial sections, procumbent body ray cells were observed, with one to up to four rows of upright and/or square marginal cells, and storied axial parenchyma (Figure 2III c). Furthermore, simple perforation plates and alternate minute (≤4 μm) intervessel pits were observed (Figure 2III c), and the presence of vascular/vasicentric tracheids, thin- to thick-walled fibers, and vasicentric axial parenchyma was registered. As reported by Waly (1999) three sections can be distinguished in the genus *Tamarix*: *Tamarix*, *Oligadenia*, and *Polyadenia*. According to Baum classification (Baum, 1978), *Tamarix nilotica* (Ehrenb.) Bunge, *T. mannifera* (Ehrenb.) Bunge, *Trichogalumna arborea*, and *T. aphylla* are species belonging to the *Tamarix* section, but Boulos., 1995 referred both *T. mannifera* and *T. arborea* as conspecific to *T. nilotica*. (Waly, 1999). Nowadays, *T. mannifera* is considered a heterotypic synonym of *T. nilotica* (Taxonomy – GRIN-Global Web v 1.10.4.1, n.d.).

In any case, even if consulting references that consider the two species as distinct, anatomical features led to *T. mannifera*. Inside Wood database description does not mention the crystal presence in cells for *T. mannifera*. On the contrary, in Waly's dichotomous key (Waly, 1999) crystals are assumed to be a discriminating character between *T. nilotica* and *T. mannifera*, being present in the first one and absent in the latter. Polarized microscopy observation confirmed the absence of crystals in the analyzed wood sample (Figure 2III d).

Following Waly's key, other species such as *T. aphylla* and *Tamarix tetragyna* can be excluded, based on the observed features. In fact, vessel frequency did not exceed 20 per square millimeter, largest tangential vessels diameter was larger than 100 μm, ray width was up to 10 cells and their height commonly exceeded >1 mm, and not only thick-walled fibers were observed. Most of the detected characters thus might suggest *T. mannifera*, if it will be considered as a separate species from *T. nilotica* (World Flora Online, Kew science – plantsoftheworldonline.org).
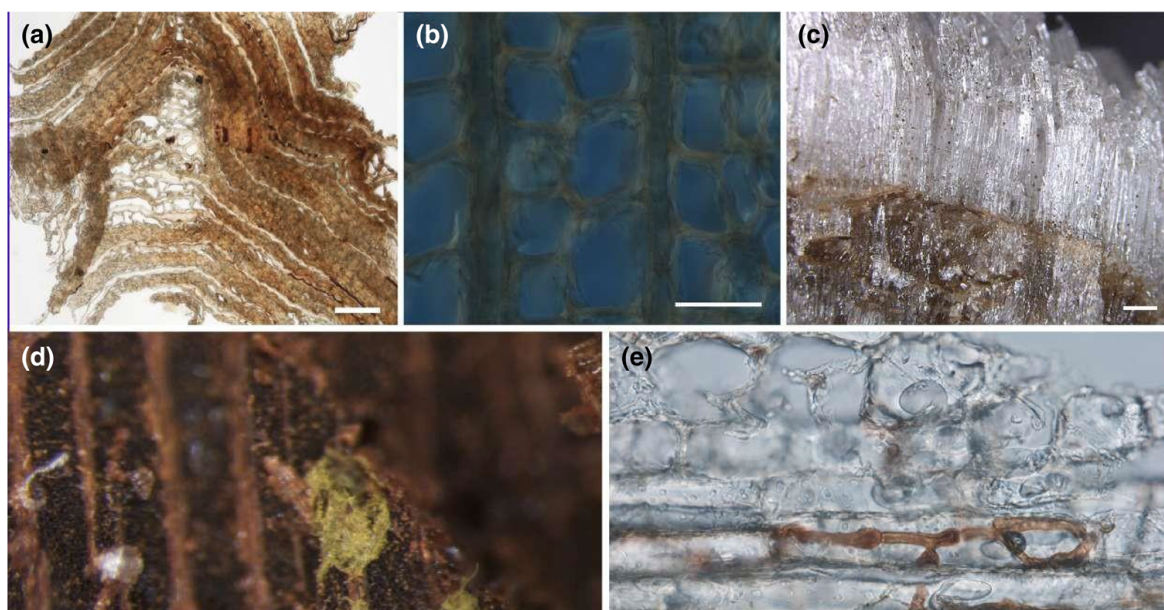
NEW DATA ON RELEVANT ANCIENT EGYPTIAN WOODEN ARTIFACTS: IDENTIFICATION OF WOODEN SPECIES AND STUDY OF THE STATE OF CONSERVATION WITH MULTIDISCIPLINARY ANALYSES

11

I

II

FIGURE 3 **I** Anthropoid coffin (ID number SR3/643), connection: Tamarisk, Tamarix gennessarensis Zoh. (a) Transverse section at stereo microscope showing semi-ring porous wood, vessels mostly solitary, seldom in multiples of 2–4 or clusters, tangential diameter of largest vessels 110–120 μm. (b) Transverse section at optical microscope. Fibres thin to thick walled. (c)(d) Tangential sections. (c) Pluriseriate rays, 2–6 seriate, 6/mm ca., height < 1 mm. Stereo microscope. (d) Pluriseriate ray with sheet cells. Optical microscope. (e)(f) Radial sections. (e) Vessels with simple perforation plates, mean vessel element length ≤ 350 μm, axial parenchyma and/or vessel elements storied. Stereo microscope. (f) Heterocellular ray with procumbent, square, and upright cells mixed throughout the ray. Optical microscope. Scale bars: a = 500 μm, b = 20 μm, c, e = 100 μm, d, f = 50 μm. **II** (a) and (b) anthropoid coffin. (c) Wooden statue observed by stereo microscope. (d) and (g) Wooden statue. (e) Box of Padimen son (body). (f) Box of Padimen son (connection). (a, b, e) Optical micrographs. (c, d) stereomicroscope images. Different forms of degradation: (a) Severe deformation of wood structure. (b) Loss of cellulose birefringence detectable at polarized light microscopy. (c) Presence of salt crystals in wood. (d) Fungi colonization on wood surface. (e) Fungi colonization in the depth of wood: hyphae passing through the ray cells. Scale bars: a = 100 μm, b = 50 μm, c = 500 μm, d = 200 μm, e = 20 μm.

The wood anatomical study of the connection of anthropoid wooden coffin led to the identification of *Tamarix gennessarensis* Zoh. according to Inside Wood and Fahn et al. 1986. A ring porous/semi-ring porous structure of wood was observed, with largest vessels of ca. 110–120 μm wide, mostly solitary, some in multiples of 2–4 or in clusters (Figure 3I a), characterized by small intervessel pits (4.6–4.9 μm). The vessel frequency was ca. 20 per square millimeter. Fibres thin to thick walled were observed (Figure 3I b). The rays were 2–6 seriate, less than 1 mm in height, with a frequency of ca. 6/mm (Figure 3I c, d). The presence of sheet cells and procumbent, square, and upright cells mixed throughout the ray, and square/upright cells at rays' margins were highlight in longitudinal sections. Mean vessels' length was ≤ 350 μm. Simple perforation plates, axial parenchyma, and/or vessel elements storied were also observed. Finally, it has to be reported that rays/axial elements were irregularly storied, and no prismatic crystals were detected (Figure 3I d-f). The species *T. gennessarensis* is currently accepted, it is reported as native of an area that goes from Anti-Lebanon to NE Israel (*Tamarix gennessarensis*, n.d. Zohary Plants of the World Online Kew Science).

Tamarix (tamarisk) species grow in salty locations, riversides, or wadis where water flows from time to time (Liphschitz, 1998). Main properties of wood are light color, medium density, and medium hardness. It is highly represented in ancient Egypt objects, often identified, along with sycomore and cedrus, in coffins, sculptures, bows, and other artifacts (Abdrabou et al., 2020; Cartwright & Taylor, 2008; Gale et al., 2000; Giachi et al., 2020).

Micro-morphological characterization of wood

The microscopic patterns of deterioration were determined by studying wood through stereo, optical, and electronic microscopes. The examined samples exhibited different degradation levels, starting from the good preservation state of box connection, which permitted obtaining good thin sections without any pre-treatment, to severe degradation degree of the statue, difficult to cut even after resin embedding. Almost all wood samples coming from the outer surfaces of the objects had numerous cracks and fractures. In particular, the wood of the statue appeared very fragile and brittle, difficult to manage due to its tendency of cracking (Figure 3II a), whereas cells appeared well preserved in box connection and body. Intermediate state of preservation was found for wooden coffin body and its connection. Even if from a macroscopic point of view it seemed in good condition, cutting revealed a quite brittle structure, with separation of cells due to the partial loss of middle lamella. The cellulose depletion was highlighted at polarized light (Figure 3II b).

The formation of salt crystals on the wooden surfaces was visible on the statue (Figure 3II c). The migration of salts into wood may have occurred during burial conditions; the interaction of wood surfaces with limestone, gypsum, sodium chloride, and moisture is proposed as a cause of chemical degradation and probably accelerated the wood deterioration (Blanchette et al., 1994).

The presence of fungi, probably referrable to a recent attack, was detected in most of the artifacts, especially in the statue and box body. A colonization of wooden surface in the statue ascribable to fungi, with greenish conidia clearly observed in Figure 3II d. OM observations revealed the presence of fungal hyphae inside the wooden cells (Figure 3II e).

Investigations of wooden objects from ancient Egypt in museums often revealed a number of different types of biological degradation and non-biological deterioration processes that have affected the various woods. These include wood decay from various types of fungi including brown and soft rot, as well as a chemical corrosion of wood by salts (Fadl et al., 2013; Geweely, 2006; Giachi et al., 2020).

Fourier transform infrared spectroscopy (FTIR)

FTIR highlighted the changes in the relative composition of chemical compounds compared to fresh woods, indicating the decay degree. Furthermore, the comparison between different peaks within the same spectrum allowed the semiquantitative analysis (Zidan et al., 2016). In general, O-H stretching absorption bands (around $3,400 \text{ cm}^{-1}$) and C-H absorption bands (around $2,927 \text{ cm}^{-1}$) gave the different contributions of all the chemical components (Bodirlau, 2009; Shi et al., 2012).

Two important peaks appeared at bands 1730–1740 and 1640 cm^{-1} that are attributed to C=O of hemicellulose and H_2O absorption, respectively, as described by Ray et al. (2012) and Picollo et al. (2011). Absorption bands at $1610–1500 \text{ cm}^{-1}$ are characteristic for lignin, whereas the $1,590–1,610 \text{ cm}^{-1}$ bands refer to aromatic C=C stretching (Syringyl > Guaiacyl). Bands at $1505–1515 \text{ cm}^{-1}$ refer to aromatic C=C stretching (Huang et al., 2012), whereas the absorption bands at $1460–1470 \text{ cm}^{-1}$ refer to C-H bending bands in cellulose and hemicellulose (Pucetaite, 2012). The absorption bands at $1346–1384 \text{ cm}^{-1}$ refer to C-H and O-H bending bands in cellulose and hemicellulose (Pucetaite, 2012). The C-O stretching band for lignin (Guaiacyl only) and hemicellulose is at $1245–1270 \text{ cm}^{-1}$ (Esteves et al., 2013). The band at 1205 cm^{-1} refers to O-H bending for hemicellulose and cellulose, C-O stretching for cellulose, and C-H bending in plane for lignin (Guaiacyl) at 1140- cm^{-1} (Bodirlau, 2009). C-O stretching for hemicellulose and cellulose at $1060–1117 \text{ cm}^{-1}$ (Ray et al., 2012), aromatic C-H bending out of plane for lignin at (800–875) and C-H rocking for cellulose at (800–950) (Huang et al., 2012; Pucetaite, 2012).

The main changes occurred in the wood chemical compounds in the area around $1,000–1800 \text{ cm}^{-1}$ (Popescu et al., 2007). The spectrum of the wooden coffin was similar to that of sound wood as a result of a good preservation; only the peak around $3,300–3,400 \text{ cm}^{-1}$ showed a decrease in O-H stretching band (Figure 4c); this was mainly due to a water loss for the dry storage conditions compared to the standard sample (*Tamarix gennessarensis*). In the wooden box, the peak at 1738 cm^{-1} was attributed to the C=O (acetyl) groups in xylan (a type of hemicellulose), and it is often observed to have decreased in intensity or been completely lost if compared to the standard sample (*Ficus sycomorus*) (Figure 4b). This is because the acetyl groups are readily hydrolyzed to acetic acid, and it does not necessarily represent degradation of the polymers (Darwish et al., 2013). On the other hand, FTIR analysis of the wooden statue showed significant changes in the chemical composition of wood due to a severe deterioration state of wood (Figure 4a). Four major differences between the archaeological sample and control sample (*Acacia nilotica*) were observed: (I) Decrease in the intensity band of
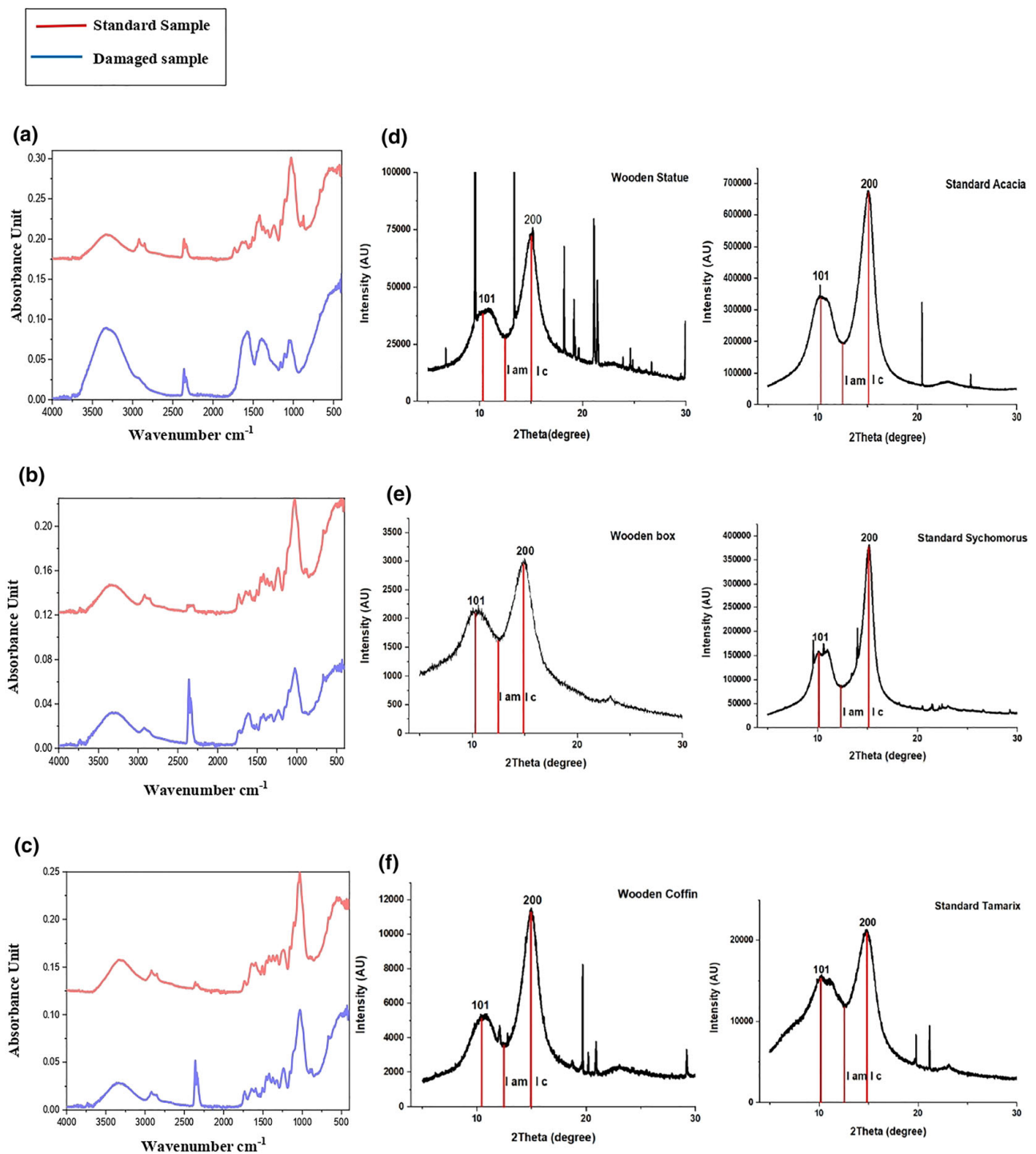
FIGURE 4 FTIR spectra & XRD patterns for old wood samples compared with standard wood samples Notes: (a) FTIR spectra for the wooden statue compared with the standard sample (Acacia nilotica). (b) FTIR spectra for the wooden box compared to the standard sample (Ficus sycomorus). (c) FTIR spectra for the wooden coffin compared to the standard sample (Tamarix gennessarensis),XRD (d) Wooden statue compared to A. nilotica as the standard sample. (e) Wooden box compared to F. sycomorus as a standard sample. (f) Wooden coffin compared to Tamarix gennessarensis as a standard sample.

unconjugated C=O stretching around ($1730 \ cm^{-1}$) in the decayed sample; this was explained by the decrease in hemicellulose amount in archaeological sample. (II) Decrease in the intensity band of water absorption around ($1{,}640 \ cm^{-1}$) and decrease in O-H stretching band around ($3{,}300–3{,}400 \ cm^{-1}$); this was due to the water loss and the dry storage conditions. (III) Decrease in C=C stretching band around ($1{,}508 \ cm^{-1}$) due to the loss of lignin according to fungal

NEW DATA ON RELEVANT ANCIENT EGYPTIAN WOODEN ARTIFACTS: IDENTIFICATION OF WOODEN SPECIES AND STUDY OF THE STATE OF CONSERVATION WITH MULTIDISCIPLINARY ANALYSES

15

T A B L E 2   Values of $I_{(200)}$, $I_{(am)}$, and X were obtained for archaeological wooden samples and standard woods

Wooden samples	$I_{(200)}$ (AU)	I_{am} (AU)	X (crystallinity index of cellulose)
Wooden statue	73,000	30,000	58.9%
Standard (*Acacia nilotica*)	680,000	200,000	70.5%
Wooden box	3,000	1750	41.6%
Standard (*Ficus Sycomore*)	375,000	90,000	76.0%
Wooden coffin	21,000	11,000	47.6%
Standard (*Tamarix gennessarensis*)	11,500	3,700	67.8%

degradation (Geweely, 2011; Kubovský et al., 2020). (IV) Decrease in C-O-C stretching bands around (1,160 cm^{-1}); this indicates the advanced cellulose chain breaking and the depolymerization occurrence (Kubovský et al., 2020).

X-ray diffraction (XRD)

The comparison between the cellulose crystallinity of the archaeological wooden samples and the standard samples of the same wood type indicated a decrease in the crystalline index of the ancient samples (Figure 4 d,e,f and Table 2). The crystallinity decreases in the decayed cellulose are linked to biotic and abiotic decay phenomena, both microbiological or due to weathering conditions. A loss in crystallinity with increasing decay was indicated by a decreasing depth of the 'trough' between the two peaks in the archaeological sample (Table 2). The use of XRD to examine the cellulose loss in archaeological wood was already demonstrated by Giachi et al., 2003 and Li et al., 2014. In addition, XRD analysis can underestimate the amount of cellulose if it is present in a noncrystalline state, having been degraded to some extent (Li et al., 2014). The major benefit of applying XRD to determine inorganic components is that it can distinguish crystal structures, in contrast to SEM–EDX, and XRF where only an elemental composition is obtained. This may provide valuable information for informing strategies to remove such compounds before conservation or for predicting how they might behave with changing environmental conditions (Sandström et al., 2002; Shen et al., 2018).

CONCLUSION

The different investigations (optical microscope observation of thin sections, SEM, FTIR, and XRD) carried out on the three ancient Egyptian wooden artifacts (a wooden statue, a wooden box, and wooden coffin) of great historical value were useful to identify the wood species and to establish the typology and the extent of the deterioration of the wood. In particular, the wooden coffin body was made of *Cedrus* sp., whereas connections were of *Tamarix gennessarensis*. The body of wooden box was made of *Ficus sycomorus*, and the connections of *Tamarix mannifera*. The wooden statue was made of *Vachellia nilotica* wood. This statue suffers from a severe deterioration due to bad burial conditions. Visual assessment and investigation of the surface morphology revealed several aspects of deterioration of the coffin surface, such as cracks; presence of salt crystals, hyphae, and spores; and a separation between the wood layers that require conservation. The analysis using FTIR allowed to know the changes in the wood chemical compounds. The significant changes in the chemical composition of wood observed for the wooden statue was probably due to a severe deterioration state of wood. Moreover, XRD analysis showed a decrease in the crystalline index of the archaeological samples,

probably due to a microbial damage or weathering conditions. Further analysis including more samples will be performed for understanding the decay pattern of different wood components.

DATA AVAILABILITY STATEMENT
In our case, Data are available within the article or its supplementary materials.

ORCID
Neveen Geweely https://orcid.org/0000-0002-9170-1114
Shimaa Ibrahim https://orcid.org/0000-0002-1740-7072

REFERENCES
Abdrabou, A., Abdallah, M., & Kamal, H. M. (2017). Scientific investigation by technical photography, OM, ESEM, XRF, XRD and FTIR of an ancient Egyptian polychrome wooden coffin. *Conservar Património*, *26*, 51–63. https://doi.org/10.14568/cp2017008

Abdrabou, A., Sultan, G. M., Elkader, M. A., & Kamal, H. M. (2020). Non-invasive wood identification on parts of king Horemheb's ritual couches (new kingdom). *Conservar Património*, *36*, 12–19. https://doi.org/10.14568/cp2019038

Baas, P., & Wheeler, E. A. (1998). Wood identification -a review. *IAWA Journal*, *19*, 241–264. https://doi.org/10.1163/22941932-90001528

Baum, B. B. (1978). *The genus Tamarix*. Israel Academy of Sciences and Humanities.

Blanchette, R. A. (2000). A review of microbial deterioration found in archaeological wood from different environments. *International Biodeterioration and Biodegradation*, *46*, 189–204. https://doi.org/10.1016/S0964-8305(00)00077-9

Blanchette, R. A. (2003). Deterioration in historic and archaeological woods from terrestrial sites. In R. J. Koestler, V. H. Koestler, A. E. Charola, & F. E. Nieto-Fernandez (Eds.), *Art, biology, and conservation: biodeterioration of works of art* (pp. 328–347). The Metropolitan Museum of Art.

Blanchette, R. A., Haight, J. E., Koestler, R. J., Hatchfield, P. B., & Arnold, D. (1994). Assessment of deterioration in archaeological wood from ancient Egypt. *Journal of the American Institute for Conservation*, *33-55*, 55. https://doi.org/10.2307/3179670

Boatwright, J. S., Van der Bank M, & Maurin, O. (2014). Name changes in African acacia species: Plant name changes. *Veld and Flora*, *100*, 33.

Bodirlau, C. T. (2009). Fourier Tranceform infrared spectroscopy and thermal analysis of lignocellulose fillers treated with organic anhydrites. *Romanian Journal of Physics*, *54*, 93–104.

Bouchenak-Khelladi, Y., Maurin, O., Hurter, J., & van der Bank, M. (2010). The evolutionary history and biogeography of Mimosoideae (Leguminosae): An emphasis on African acacias. *Molecular Phylogenetics and Evolution*, *57*, 495–508. https://doi.org/10.1016/j.ympev.2010.07.019

Boulos., L. (1995). *Flora of Egypt: a checklist*. Al-Hadara Publishing.

Caneva, G., Nugari, M. P., Nugari, M. P., & Salvadori, O. (2008). Processes of Biodeterioration: General Mechanisms. Chapter 1. *In Plant Biology for Cultural Heritage* (pp. 15-34). Getty Publications.

Cartwright, C. R. (2015). The principles, procedures and pitfalls in identifying archaeological and historical wood samples. *Annals of Botany*, *116*(1), 1–13. https://doi.org/10.1093/aob/mcv056

Cartwright, C. R. (2019). Identifying ancient Egyptian coffin woods from the Fitzwilliam Museum, Cambridge using scanning electron microscopy. In H. Strudwick & J. Dawson (Eds.), *Ancient Egyptian coffins. Past. Present. Future* (pp. 1–12). Oxbow Books.

Cartwright, C. R. (2020). Understanding wood choices for ancient panel painting and mummy portraits in the APPEAR project through scanning electron microscopy. In M. Svoboda & C. R. Cartwright (Eds.), *Mummy portraits of Roman Egypt: Emerging research from the APPEAR project* (pp. 16–23). J. Paul Getty Museum, Los Angeles Getty Publications.

Cartwright, C. R., & Taylor, J. H. (2008). Wooden Egyptian archery bows in the collections of the British museum. *British Museum Technical Research Bulletin*, *2*, 77–83.

Creasman, P. P. (2014). Reflections of a timber economy: The interpretation of middle kingdom ship and boat timbers. *Göttinger Misz*, *240*, 19–36.

Creasman, P. P. (2015). Exposing ancient Egyptian shipbuilders' secrets. In C. Graves-Brown (Ed.), *Egyptology in the Present* (pp. 13–38). The Classical Press of Wales. https://doi.org/10.2307/j.ctvvnbgg.6

Crivellaro, A., & Schweingruber, F. H. (2013). *Atlas of wood, bark and pith anatomy of Eastern Mediterranean trees and shrubs: with a special focus on Cyprus*. Springer-Verlag. https://doi.org/10.1007/978-3-642-37235-3

Darwish, S. S., El Hadidi, N., & Mansour, M. (2013). The effect of fungal decay on Ficus sycomorus wood. *International Journal of Conservation Science*, *4*, 271–282.

Esteves, B., Marques, A. V., Domingos, I., & Pereira, H. (2013). Chemical changes of heat treated pine and eucalypt wood monitored by ftir. *Maderas Cienc. Y Tecnology*, *15*, 245–258. https://doi.org/10.4067/S0718-221X2013005000020

Fadl, M. A., Fahmy, A. G., & Omran, W. (2013). Evaluation of cultivated and wild plant macroremains from a Predynastic temple in Hierakonpolis-upper Egypt. *International Journal of Plant & Soil Science*, *2*, 244–262. https://doi.org/10.9734/IJPSS/2013/4893

Fagg, C. W., & Mugedo, J. Z. A. (2005). Acacia nilotica (L.) Willd. ex Delile. In P. C. M. Jansen & D. Cardon (Eds.), *PROTA (Plant Resources of Tropical Africa / Ressources végétales de l'Afrique tropicale)*. Accessed 9 August 2022.

Gale, R., & Cutler, D. F. (2000). *Plants in archaeology: Identification manual of vegetative plant materials used in Europe and the southern Mediterranean to c. 1500*. Westbury and Royal Botanic Gardens.

Gale, R., Gasson, P., Hepper, N., & Killen, G. (2000). Wood. In P. T. Nicholson & I. Shaw (Eds.), *Ancient Egyptian materials and technology* (pp. 334–371). Cambridge University Press.

Galotta, G. (1999). *Studi di caratterizzazione per la conservazione dei manufatti lignei provenienti dalle aree di scavo vesuviane*. Università degli Studi di Firenze.

Geweely, N. (2006). Non-toxic fumigation and alternative control techniques against fungal colonization for preserving archaeological oil painting microbial deterioration of archeological objects. *International Journal of Botany*, *2*, 353–362. https://doi.org/10.3923/ijb.2006.353.362

Geweely, N. S. (2022). A novel comparative review between chemical, natural essential oils and physical (ozone) conservation of archaeological objects against microbial deterioration. *Geomicrobiology*, *39*, 531–540. https://doi.org/10.1080/01490451.2022.2043959

Geweely, N. S. I. (2011). Evaluation of ozone for preventing fungal influenced corrosion of reinforced concrete bridges over the River Nile, Egypt. *Biodegradation*, *22*, 243–252. https://doi.org/10.1007/s10532-010-9391-7

Giachi, G., Bettazzi, F., Chimichi, S., & Staccioli, G. (2003). Chemical characterisation of degraded wood in ships discovered in a recent excavation of the Etruscan and Roman harbour of Pisa. *Journal of Cultural Heritage*, *4*, 75–83. https://doi.org/10.1016/S1296-2074(03)00018-9

Giachi, G., Guidotti, M. C., Lazzeri, S., Macchioni, N., & Sozzi, L. (2020). Wood identification of some coffins from the necropolis of Thebes held in the collection of the Egyptian Museum in Florence. *Journal of Cultural Heritage*, *9*, 340–346. https://doi.org/10.1016/j.culher.2020.09.007

Giachi, G., Guidotti, M. C., Lazzeri, S., Sozzi, L., & Macchioni, N. (2016). Wood identification of the headrests from the collection of the Egyptian Museum in Florence. *Journal of Archaeological Science: Reports*, *9*, 340–346. https://doi.org/10.1016/j.jasrep.2016.08.027

Giordano, G. (1981). *Tecnologia del legno* (Vol. 1). UTET.

Giordano, G. (1997). *Antologia del legno*. Consorzio Legnolegno.

Haddad, W. A. (2011). Classification and nomenclature of the genus acacia (Leguminosae), with emphasis on Africa. *Dendron*, *43*(2011), 34–43.

Hamed, S. A. M., Ali, M. F., & El Hadidi, N. M. N. (2012). Using SEM in monitoring changes in archaeological wood: A review. In A. Méndez- Vilas (Ed.), *Current Microscopy Contributions to Advances in Science Technology* (pp. 1077–1084). Spain Formatex Research Center.

Huang, Y., Wang, L., Chao, Y., Nawawi, D. S., Akiyama, T., Yokoyama, T., & Matsumoto, Y. (2012). Analysis of lignin aromatic structure in wood based on the IR spectrum. *Journal of Wood Chemistry and Technology*, *32*, 294–303. https://doi.org/10.1080/02773813.2012.666316

Jenkins, N., & Ross, J. (1980). *The boat beneath the pyramid. King Cheop's royal ship*. Holt Rinehart and Winston.

Ju, X., Bowden, M., Brown, E. E., & Zhang, X. (2015). An improved X-ray diffraction method for cellulose crystallinity measurement. *Carbohydrate Polymers*, *123*, 476–481. https://doi.org/10.1016/j.carbpol.2014.12.071

Killen, G. (2017). *Ancient Egyptian furniture* (2nd ed.). Oxbow Books.

Kubovský, I., Kačíková, D., & Kačík, F. (2020). Structural changes of oak wood Main components caused by thermal modification. *Polymers (Basel)*, *12*, 485. https://doi.org/10.3390/polym12020485

Kyalangalilwa, B., Boatwright, J. S., Daru, B. H., Maurin, O., & van der Bank, M. (2013). Phylogenetic position and revised classification of acacia s.l. (Fabaceae: Mimosoideae) in Africa, including new combinations in Vachellia and Senegalia. *Botanical Journal of the Linnean Society*, *172*, 500–523. https://doi.org/10.1111/boj.12047

Li, M. Y., Fang, B. S., Zhao, Y., Tong, T., Hou, X. H., & Tong, H. (2014). Investigation into the deterioration process of archaeological bamboo strips of China from four different periods by chemical and anatomical analysis. *Polymer Degradation and Stability*, *109*, 71–78. https://doi.org/10.1016/j.polymdegradstab.2014.06.022

Liphschitz, N. (1998). Timber identification of wooden egyptian objects in museum collections in Israel. *Tel Aviv*, *25*, 255–276. https://doi.org/10.1179/tav.1998.1998.2.255

Lucas, A. (1959). *Ancient Egyptian materials and industries*. Edward Arnold LTD.

Meiggs, R. (1982). *Trees and timber in the ancient Mediterranean world*. Clarendon Press.

Melchiorre, C., Dello Ioio, L., Ntasi, G., Birolo, L., Trojsi, G., Cennamo, P., Barone Lumaga, M. R., Fatigati, G., Amoresano, A., & Carpentieri, A. (2020). A multidisciplinary assessment to investigate a XXII dynasty wooden coffin. *International Journal of Conservation Science*, *11*, 25–38.

Nardi Berti, R., Fioravanti, M., & Macchioni, N. (2006). *La struttura anatomica del legno ed il riconoscimento dei legnami italiani di più corrente impiego*. CNR-IVALSA.

Nilsson, T., & Daniel, G. (1989). Structure and the aging process of dry archaeological wood. In R. M. Rowell & J. R. Barbour (Eds.), *Archaeological Wood - Properties, chemistry, and preservation* (pp. 67–86). American Chemical Society. https://doi.org/10.1021/ba-1990-0225.ch003

Nisbet, R. (1982). Analysis of the different kinds of wood of Kha tomb in the Egyptian Museum in Turin. *Italia forestale e montana*, *37*(2), 89–98.

Orwa, C., Mutua, A., Kindt, R., Jamnadass, R., & Simons, A. (2009). Agroforestree Database: A tree reference and selection guide version 4.0.

Picollo, M., Cavallo, E., Macchioni, N., Pignatelli, O., Pizzo, B., Santoni, I., Maier, M. S., & Sas, D. (2011). Spectral characterisation of ancient wooden artefacts with the use of traditional IR techniques and ATR device: A methodological approach. *E-Preservation Science*, *8*, 23–28.

Plaisier, J. R., Luca, N., Lara, G., Paz, R. S. M. E., Renzo, B., & Andrea, L. (2017). The X-ray diffraction beamline MCX at Elettra: A case study of non-destructive analysis on stained glass. *ACTA IMEKO*, *6–3*, 71–75. https://doi.org/10.21014/acta_imeko.v6i3.464

Popescu, C. M., Dobele, G., Rossinskaja, G., Dizhbite, T., & Vasile, C. (2007). Degradation of lime wood painting supports. Evaluation of changes in the structure of aged lime wood by different physico-chemical methods. *Journal of Analytical and Applied Pyrolysis*, *79*, 71–77. https://doi.org/10.1016/j.jaap.2006.12.014

Pucetaite, M (2012). Archaeological wood from the Swedish warship vasa studied by infrared microscopy, Lund University. http://lup.lub.lu.se/student-papers/record/2297786 (accessed November 2, 2021).

Ray, R., Majumder, N., Chowdhury, C., & Jana, T. K. (2012). Wood chemistry and density: An analog for response to the change of carbon sequestration in mangroves. *Carbohydrate Polymers*, *90*, 102–108. https://doi.org/10.1016/j.carbpol.2012.05.001

Richter, H. G., & Dallwitz, M. (2000). *Commercial timbers: Descriptions, illustrations, identification, and information retrieval*, Delta. https://www.delta-intkey.com/wood/en/index.htm

Romagnoli, M., Galotta, G., Antonelli, F., Sidoti, G., Humar, M., Kržišnik, D., Čufar, K., & Davidde Petriaggi, B. (2018). Micro-morphological, physical and thermogravimetric analyses of waterlogged archaeological wood from the prehistoric village of gran Carro (Lake Bolsena-Italy). *Journal of Cultural Heritage*, *33*, 30–38. https://doi.org/10.1016/j.culher.2018.03.012

Sandström, M., Jalilehvand, F., Persson, I., Gelius, U., Frank, P., & Hall-Roth, I. (2002). Deterioration of the seventeenth-century warship vasa by internal formation of sulphuric acid. *Nature*, *415*, 893–897. https://doi.org/10.1038/415893a

Schwarze, F. W. M. R. (2007). Wood decay under the microscope. *Fungal Biology Reviews*, *21*, 133–170. https://doi.org/10.1016/j.fbr.2007.09.001

Shen, D., Li, N., Fu, Y., Macchioni, N., Sozzi, L., Tian, X., & Liu, J. (2018). Study on wood preservation state of Chinese ancient shipwreck Huaguangjiao I. *Journal of Cultural Heritage*, *32*, 53–59. https://doi.org/10.1016/j.culher.2018.01.009

Shi, J., Xing, D., & Li, J. (2012). FTIR studies of the changes in wood chemistry from wood forming tissue under inclined treatment. In Y. Guohui (Ed.), *2012 International Conference on Future Energy, Environment, and Materials, Energy Procedia* (Vol. 16, Part B, pp. 758–762). Elsevier Ltd. https://doi.org/10.1016/j.egypro.2012.01.122

Tamarix gennessarensis. (n.d.). Zohary|Plants of the World Online|Kew Science. http://www.plantsoftheworldonline.org/taxon/urn:lsid:ipni.org:names:828113-1 (accessed December 30, 2020).

Tamburini, D., Łucejko, J. J., Pizzo, B., Mohammed, M. Y., Sloggett, R., & Colombini, M. P. (2017). A critical evaluation of the degradation state of dry archaeological wood from Egypt by SEM, ATR-FTIR, wet chemical analysis and Py (HMDS)-GC-MS. *Polymer Degradation and Stability*, *146*, 140–154. https://doi.org/10.1016/j.polymdegradstab.2017.10.009

Taxonomy - GRIN-Global Web v 1.10.4.1. (n.d.). http://tngrin.nat.tn/gringlobal/taxonomydetail.aspx?id=80022 (accessed December 30, 2020).

Timar, M. C., Gurau, L., Cionca, M., & Porojan, M. (2010). Wood species for the biedermeier furniture - a microscopic characterisation for scientific conservation. *International Journal of Conservation Science*, *1*, 3–12.

Waly, N. M. (1999). Wood anatomical characters of the Egyptian Tamarix L. species and its taxonomic significance. *Taeckholmia*, *19*, 115–125. https://doi.org/10.21608/taec.1999.12640

Wheeler, E. A. (2011). InsideWood - a web resource for hardwood anatomy. *IAWAJ*, *32*, 199–211. https://doi.org/10.1163/22941932-90000051

Zidan, Y., El Hadidi, N. N., & Mohamed, M. F. (2016). Examination and analyses of a wooden face at the museum storage at the faculty of archaeology, Cairo university. *Mediterranean Archaeology and Archaeometry*, *16*, 1–11.

How to cite this article: Geweely, N., Abu Taleb, A., Ibrahim, S., Grenni, P., Caneva, G., Galotta, G., Abdallah, M., Atwa, D., Plaisier, J., & Antonelli, F. (2022). New data on relevant ancient Egyptian wooden artifacts: Identification of wooden species and study of the state of conservation with multidisciplinary analyses. *Archaeometry*, 1–19. https://doi.org/10.1111/arcm.12815